

Buried *S*-Nitrosocysteine Revealed in Crystal Structures of Human Thioredoxin^{†,‡}

Andrzej Weichsel, Jacqueline L. Brailey, and William R. Montfort*

Department of Biochemistry and Molecular Biophysics, University of Arizona, Tucson, Arizona 85721

Received September 9, 2006; Revised Manuscript Received November 24, 2006

ABSTRACT: We have determined the 1.65 Å crystal structure of human thioredoxin-1 after treatment with *S*-nitrosoglutathione, providing a high-resolution view of this important protein modification and mechanistic insight into protein transnitrosation. Thioredoxin-1 appears to play an intermediary role in cellular *S*-nitrosylation and is important in numerous biological and pathobiological activities. *S*-Nitroso modifications of cysteines 62 and 69 are clearly visible in the structure and display planar cis geometries, whereas cysteines 32, 35, and 73 form intra- and intermolecular disulfide bonds. Surprisingly, the Cys 62 nitroso group is completely buried and pointing to the protein interior yet is the most readily formed at neutral pH. The Cys 69 nitroso group is also protected but requires a higher pH for stable formation. The helix intervening between residues 62 and 69 shifts by ~0.5 Å to accommodate the SNO groups. The crystallographic asymmetric unit contains three independent molecules of thioredoxin, providing three views of the nitrosated protein. The three molecules are in general agreement but display subtle differences, including both cis and trans conformers for Cys 69 SNO in molecule C, and greater disorder in the Cys 62–Cys 69 helix in molecule B. Possible mechanisms for protein transnitrosation with specific geometric requirements and charge stabilization of the nitroxyl disulfide reaction intermediate are discussed.

Nitric oxide is widely synthesized in higher eukaryotic cells for the regulation of numerous physiological processes, including blood pressure, tissue development, memory formation, cell growth, and cell death (1). Paradoxically, higher levels of NO, produced in response to inflammation and infection, may be toxic and contribute to, for example, septic shock (2) and neurodegeneration (3). The best-characterized NO-dependent signaling processes occur through binding to the heme of soluble guanylate cyclase (sGC),¹ stimulating the protein to convert GTP to cyclic GMP and initiating a cGMP signaling cascade (4). However, much of the NO produced in the cell does not lead to such complexes but rather to various nitrosations and nitrations, or to nitrite and nitrate. Many of these products may be signaling intermediates in their own right, particularly *S*-nitrosocysteine (5). For example, nitrosation (nitrosylation)² of β-Cys 93 in human hemoglobin occurs readily and is sensitive to the hemoglobin conformation, leading to the proposal that

hemoglobin delivers NO to oxygen deficient tissue, resulting in vasodilation (6). More than 100 proteins have been shown to be *S*-nitrosylated in vivo (5, 7), and a broad array of cellular functions appear to be under the influence of *S*-nitrosylation, particularly with respect to gene regulation and apoptosis. Structural and chemical insight into these protein modifications have lagged behind the biology, and only one structure of an *S*-nitrosated protein has been reported, a specialized case involving a thiol-linked heme in a nitrophorin (8). Attempts to determine the structure of *S*-nitrosohemoglobin through direct reaction with NO have led to structures with modified β-Cys 93, but with geometry more consistent with a thionitroxide modification (9, 10).

Thioredoxin has recently emerged as a central intermediary in cellular *S*-nitrosation events. All cells use thioredoxin for maintaining an appropriately reducing cytosol through oxidoreductase activities involving a Cys-Gly-Pro-Cys motif and NADPH-dependent thioredoxin reductase (11). In mammals, thioredoxin-1 is important in numerous additional activities, including cell growth, cell death, oxidative and nitrosative stress, and tissue development (12, 13). Thioredoxin-1 is overexpressed in many cancers and directly binds to many tumor-promoting proteins, including NFκB, Ref-1, AP-1, PTEN, HIF1-α, and ASK-1, and thioredoxin-1 gene disruption in mice is embryonically lethal (14). Human thioredoxin-1 (hTrx) is readily *S*-nitrosated (nitrosylated) both in vitro and in vivo (15–18), and high levels of hTrx lead to increased levels of protein *S*-nitrosylation in cell culture or heart tissue, while low levels of hTrx lead to low levels of *S*-nitroso protein (16, 17). *S*-Nitrosated hTrx (hTrx-SNO) can directly transnitrosate caspase-3, leading to inactivation of this important protein (18), and can be taken up by heart tissue, where it exerts a cardioprotective effect (17).

[†]This work was supported by NIH Grant HL62969. Diffraction measurements at BioCars Sector 14, Advanced Photon Source, Argonne National Laboratory, Argonne, IL, were supported by DOE Contract W-31-109-Eng-38 and NCRR Grant RR07707.

[‡]Coordinates and structure factors have been deposited in the Protein Data Bank (entries 2HXX, 2IFQ, 2IY, and 2HSH).

* To whom correspondence should be addressed. Telephone: (520) 621-1884. Fax: (520) 621-1697. E-mail: montfort@email.arizona.edu.

¹ Abbreviations: sGC, soluble guanylate cyclase; hTrx, human thioredoxin-1; SNO, nitrosated sulfur; hTrx-SNO, *S*-nitrosated hTrx; GSH, glutathione; GSNO, *S*-nitrosoglutathione.

² Two nomenclatures are employed for the SNO group formation: nitrosation and nitrosylation. The first emphasizes classical chemical nomenclature and the addition of an NO⁺ equivalent to sulfur. The second is consistent with classical modifications in biology (phosphorylation, glycosylation, etc.) and does not assume a chemical mechanism in the formation of the group. Here, we use *S*-nitrosation when emphasizing the transnitrosation chemistry that was employed and *S*-nitrosylation when referring to biological modifications.

The mechanism by which cellular nitrosothiols initially form is not known, but it has been proposed to occur through reaction of free thiols with N_2O_3 and other products of nitric oxide and oxygen, through direct reaction with thiol followed by one-electron oxidation by oxygen or metal centers, or through direct reaction with thiyl radicals generated by one-electron oxidation. Glutathione (GSH), at 1–10 mM, is the most prominent initial cytosolic target, yielding *S*-nitroso-glutathione (GSNO) as the reaction product. Once formed, the nitroso group (formally NO^+) can be transferred between thiols, ultimately residing on those thiols providing stability for the SNO moiety. Competing with this process is SNO degradation, which can occur spontaneously or via several other processes, including reduction of GSNO by GSNO reductase/formaldehyde dehydrogenase (19). An understanding of the dynamics surrounding nitrosothiol flux in vivo has not yet been realized, but it is clear that the majority of isolatable nitrosothiol groups in the cell reside on proteins (19, 20). Here, we provide the first view of a transnitrosated protein, hTrx-SNO.

MATERIALS AND METHODS

Materials. Recombinant wild-type and C73S mutant human thioredoxin-1 (hTrx) were expressed in *Escherichia coli* without purification tags and isolated by column chromatography as previously described (21, 22). Mass spectral analyses of the wild-type protein indicated the N-terminal methionine was largely, but not completely, processed away during expression, leaving perhaps 10% unprocessed protein. *S*-Nitrosoglutathione (GSNO) was prepared from reduced L-glutathione and sodium nitrite (Sigma) as described previously (23) and recrystallized from a water/acetone mixture. Other reagents were purchased from Sigma unless otherwise noted.

Quantifying hTrx-SNO Formation. *S*-Nitrosation of hTrx was examined under a variety of conditions. The variables that were examined included protein and GSNO concentrations, pH, molar ratios, time, temperature, and the presence or absence of glutathione. In the first series of experiments, the concentration of hTrx was varied from 10 to 200 μM and mixed with 1–10-fold molar excess of GSNO on ice and in the dark. The reactions were performed in either 100 mM potassium phosphate buffer (pH 7.0) or 100 mM sodium glycine buffer (pH 9.0), each supplemented with metal chelators diethylenetriaminepentaacetic acid (DTPA) and neocuprione, 50 μM each. After equilibration for 30 min to 2 h, excess GSNO was removed by repeated ultrafiltration using a Centricon filter with a 10 kDa cutoff.

The SNO contents of the retentate and filtrate were determined using the Griess–Saville method (24, 25). In brief, a standard curve was generated using sodium nitrite and Griess reagent. Portions of the retentate and last filtrate were supplemented with fresh Griess reagent and incubated for 10 min. These solutions displayed zero absorbance at 540 nm, indicating that the nitrite concentration was less than 1 μM . Addition of excess mercury(II) acetate (from a 20 mM solution) converted SNO to nitrite, leading to reaction with Griess reagent and absorbance at 540 nm. The final concentration of hTrx-bound SNO was calculated as the difference between the retentate and filtrate SNO concentrations, and the concentration of hTrx was determined by

Table 1: Representative SNO Measurements

[hTrx] (μM)	[GSNO] (μM)	[GSH] (μM)	pH ^a	SNO/hTrx molar ratio	
				Griess/Saville	A ₃₃₅
10	50	0	9.0	1.96	—
10	50	0	7.0	0.89	—
10	50	1000	9.0	0.56	—
10	50	1000	7.0	0.29	—
1500	15000	0	9.0	2.13	2.19
600	1000	0	7.0	1.06	1.19

^a pH values of 5.6 and 4.0 were also examined but display no SNO formation.

absorbance at 280 nm ($\epsilon_{280} = 7266 \text{ M}^{-1} \text{ cm}^{-1}$). A somewhat jagged A_{280} band was found for the material, most likely due to disulfide bond formation or multiple environments for the single tryptophan residue.

In experiments designed to assess *S*-nitrosation of hTrx in the presence of GSH, 10 μM hTrx was mixed with 50 μM GSNO and 1 mM GSH. After incubations ranging from 2 to 24 h, at 0 or 37 °C, and pH 7 or 9, hTrx-SNO and GSNO were separated by ultrafiltration and SNO content determined as described above. Of these variables, only pH led to a change in the SNO content of hTrx.

***S*-Nitrosation for Crystallization.** Preparative quantities of hTrx-SNO for crystallization were obtained by mixing 200 μL of hTrx (42 mg/mL) and 100 μL of 50 mM GSNO in 700 μL of either sodium phosphate buffer (50 mM, pH 7.0) or sodium glycine buffer (50 mM, pH 9.0), supplemented with 50 μM neocuprione and 50 μM DTPA. After equilibration for 90 min on ice in the dark, hTrx-SNO and GSNO were separated by repeated washing of the sample with 20 mM phosphate buffer (pH 7.0) using ultrafiltration (10 kDa cutoff Centricon filter). The SNO contents in the retentate and the last filtrate were determined either by the Griess–Saville method or spectroscopically at 335 nm ($\epsilon_{335} = 927 \text{ M}^{-1} \text{ cm}^{-1}$) (26). This material exhibited SNO content similar to that prepared at lower concentrations (Table 1). The final hTrx-SNO material was concentrated to $\sim 1.5 \text{ mM}$ and stored in 100 μL aliquots at -80°C .

S-Nitrosation of hTrx with similar results was also obtained by combining equivolume solutions of hTrx (42 mg/mL) with a freshly prepared mixture of 0.5 M Cys-HCl and 0.5 M sodium nitrite in 0.5 M sodium glycine buffer (pH 9). This sample was kept in the dark on ice for 30 min followed by washing using ultrafiltration.

Crystallization. The hTrx-SNO crystals were obtained using the hanging drop method by combining 2 μL of hTrx-SNO ($\sim 1.5 \text{ mM}$) with 2 μL of 32% (w/v) PEG 1500 buffered with 50 mM sodium phosphate (pH 7) and equilibrating at room temperature against the same solution in the well. The morphology for the rod-shaped crystals, which grew spontaneously to dimensions of approximately 0.1 mm \times 0.1 mm \times 0.7 mm, was improved through macroseeding into a solution slightly lower in protein concentration ($\sim 1.2 \text{ mM}$) and lower in PEG 1500 (16%), again buffered in 50 mM sodium phosphate (pH 7). The crystals were isomorphous with those previously obtained from a 2-methyl-2,4-pentanedione (MPD)/acetate solution (pH 3.8) (22), which display a rhombohedral habit and a single molecule in the asymmetric unit. Flash-freezing of the new crystals in liquid nitrogen led to unacceptable streaking in the diffraction

Table 2: Crystallographic Data

	hTrx-SNO	hTrx-SNO	hTrx-SNO	C73S
data set	I	II	III	
PDB entry	2HXX	2IFQ	2IIY	2HSB
	Crystal Preparation			
pH of S-nitrosation	9.0	9.0	7.0	not applicable
cryoprotection	ethanol	ethanol	PEG 4K	MPD
unit cell				
<i>a</i> (Å)	116.4	116.1	66.9	66.1
<i>b</i> (Å)	25.7	25.8	26.2	26.4
<i>c</i> (Å)	86.0	85.9	51.3	51.1
β (deg)	98.2	98.0	95.0	95.5
space group	C2	C2	C2	C2
<i>Z</i>	12	12	4	4
<i>V_M</i> ^a (Å ³ /Da)	1.82	1.82	1.92	1.90
	Data Collection			
X-ray source	RAXIS	14BM-C	RAXIS	RAXIS
wavelength (Å)	1.5418	0.9002	1.5418	1.5418
resolution (Å)	1.65	1.20	1.70	1.35
no. of observed reflections	77519	396551	38295	53737
no. of unique reflections	29229	79717	9820	16046
completeness (%) ^b	99.0 (99.9)	97.1 (98.4)	98.0 (94.0)	86.2 (50.6)
<i>I</i> / σ (<i>I</i>) ^b	16.1 (3.6)	9.1 (3.3)	20.8 (4.2)	30.1 (3.9)
<i>R</i> _{merge} ^b	0.04 (0.14)	0.07 (0.24)	0.04 (0.19)	0.03 (0.14)
	Structure Refinement			
<i>R</i> _{cryst} ^b	0.19 (0.31)	0.18 (0.16)	0.21 (0.31)	0.12 (0.21)
<i>R</i> _{free} ^b	0.24 (0.34)	0.21 (0.18)	0.24 (0.32)	0.17 (0.30)
rmsd for bonds (Å)	0.021	0.021	0.019	0.018
rmsd for angles (deg)	1.9	1.8	2.0	1.6

^a *V_M* is the Matthews coefficient. ^b Overall (outer shell).

pattern. Soaking of the crystals for 24 h in 35% PEG 1500 buffered at pH 4.0 and flash-freezing led to improved diffraction and data set hTrx-SNO III (Table 2).

A more dramatic improvement in diffraction quality was achieved by transferring the hTrx-SNO crystals to 100% ethanol, equilibrating overnight and flash-freezing. The improved diffraction was a consequence of a solid-state phase transition in the crystals, which produced a new crystal form with a 3-fold larger volume and three molecules per asymmetric unit rather than one. The transformation from small to large unit cell is as follows: $a' = a + 2c$, $b' = b$, $c' = a - c$. Data were measured from two such crystals [hTRX-SNO I and II (Table 2)].

The C73S mutant was crystallized from 25% (w/v) MPD, 10 mM sodium acetate (pH 3.8), and 8% H₂O₂ through equilibration at room temperature against the same solution with 50% MPD. The crystals were flash-frozen in the mother liquor.

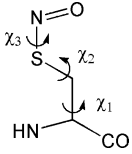
Structure Determinations. Diffraction data for hTrx-SNO (data sets I and III) and C73S were measured in house at 100 K on a Rigaku R-Axis IV⁺⁺ imaging plate system with Max-Flux confocal optics and processed with d*TREK (27) (Table 2). Diffraction data were also measured for hTrx-SNO crystals (large cell) using synchrotron radiation at APS beamline 14 BM-C (BioCARS). Data were measured at 100 K for a total of 90 min ($\lambda = 0.9$ Å), resulting in excellent data to 1.2 Å (data set II). The hTrx-SNO structure (large cell) was determined by molecular replacement using MOLREP in the CCP4 program suit (28), and wild-type hTrx as a starting model (PDB entry 1ERT) (22). Three independent protein molecules were found in the asymmetric unit, modeled with COOT (29), and refined with REFMAC5 (28). Molecules A and B form a homodimer with a noncrystallographic 2-fold axis approximately parallel to crystal-

lographic direction *b*. Molecule C constitutes half of another homodimer, of which the other monomer can be generated by the crystallographic 2-fold axis at $x = 0.5a$ and $z = 0$. The dimers are formed through disulfide bond linkage between Cys 73 of each monomer. The active site cysteines, Cys 32 and Cys 35, also form disulfide bonds, and Cys 62 and Cys 69 are nitrosated in all three molecules. Bond lengths and bond angles for SNO were restrained during refinement to the values found in small-molecule crystal structures (30, 31), and the SNO group was restrained to be planar (Table 3). Minor alternate SNO conformations were found for Cys 62 molecule A and Cys 69 molecule C.

We attempted to extend the resolution of this structure using synchrotron radiation; however, this led to photoreduction in the crystal. Both SNO and disulfide modifications proved to be sensitive, and all displayed evidence of photoreduction and bond cleavage. The refined structure of the frozen crystal retained the SNO-induced changes in protein conformation, and the higher resolution was useful for interpreting these changes in addition to providing clear evidence of photoreduction. Only Cys 69 in molecules A and C retained any indication of SNO, and these were included in the model with partial occupancy, with the Cys 69-SNO group in molecule C adopting a trans conformation. The disulfide bonds were all modeled as a mixture of reduced and oxidized species. A similar photoreduction of the active site disulfide bond in *Trichomonas vaginalis* thioredoxin has been reported (32).

The structure of hTrx-SNO III (small cell) was determined by difference Fourier analysis using the unmodified structure. The structure reveals that treatment with GSNO at pH 7 leads to a fully nitrosated Cys 62 with cis geometry ($\chi_1 = -65^\circ$, $\chi_2 = -82^\circ$, and $\chi_3 = 1^\circ$). Cys 69 was almost completely free of modification and did not display the local expansion

Table 3: SNO Geometry



	torsional angle (deg)			bond angle (deg)		bond length (Å)	
	χ_1	χ_2	χ_3	C-S-N	S-N-O	S-N	N-O
restraint ^a	NA	NA	0/180	100	114	1.80	1.20
Cys 62 A ^b	-53	-89	2	101	118	1.80	1.21
	-70	-166	0	100	118	1.81	1.22
B	-93	-156	-1	104	118	1.81	1.21
C	-64	-175	5	99	118	1.80	1.22
Cys 69 A	-67	-76	0	101	119	1.80	1.21
B	-64	-81	2	106	118	1.80	1.20
C ^c	-68	-72	3	103	123	1.81	1.20
	-63	-107	179	103	114	1.81	1.23

^a Value for restraint in refinement. ^b Two SNO conformations were observed: $\chi_2 = -89^\circ$ (60% occupancy) and $\chi_2 = -166^\circ$ (40% occupancy). ^c Two SNO conformations were observed: cis (70% occupancy) and trans (30% occupancy).

that accompanies nitrosation at pH 9. Active site residues Cys 32 and Cys 35 form a well-ordered disulfide bond, while Cys 73 was modeled as 50% disulfide-linked and 50% reduced. Interestingly, Cys 62-SNO occupies the minor conformation seen in molecule A of hTrx-SNO I (large cell), rotated $\sim 90^\circ$ about χ_2 with respect to the major conformation (Table 1). Possibly, rotation of Cys 62-SNO in the crystal is linked to the change in the crystal form. We also examined hTrx-SNO prepared at pH 9 in the smaller unit cell, which produced a preliminary model very similar to that for the pH 7 material, except with a prominent SNO group on Cys 69. These data were poorer in quality than those for the large unit cell and were not pursued further. Figures were prepared with SigmaPlot (SPSS, Inc., Chicago, IL), MOLSCRIPT (33), BOBSCRIPT (34), RASTER3D (35), PyMOL (W. L. DeLano, <http://www.pymol.org>), and Adobe Illustrator 9.0.

Crystal Spectroscopy. Crystal spectra were recorded using a microspectrophotometer consisting of an optical stage with focusing optics (4DXray Systems), a xenon lamp, and a CCD-based spectrophotometer (Spectral Instruments). The crystal was kept at 100 K using an Oxford cryosystem.

Gel Analyses. We examined GSNO stimulation of hTrx covalent dimer formation by Western blot analyses, using an anti-human thioredoxin antibody (BD Bioscience). Samples prepared with or without GSNO were subjected to SDS-PAGE run without reductant or prior boiling, to preserve the existing disulfide bond character in the solution. We also examined hTrx obtained from cultured HT1080 cells, a human fibrosarcoma cell line, after addition of GSNO. The cells were grown in tetracycline free media and harvested using 0.25% trypsin, as previously described (36). After being washed in phosphate-buffered saline (PBS), the cells were lysed in PBS containing 1% Triton X, 12 mM deoxycholate, 0.1% SDS, and a protease inhibitor cocktail (Sigma) and analyzed after cell debris had been pelleted and the supernatant incubated with GSNO for 3.5 h.

We also examined the biotin-switch approach for detecting hTrx-SNO (37). In brief, this approach first modifies free sulfhydryls in S-nitrosated proteins with methylmethaneth-

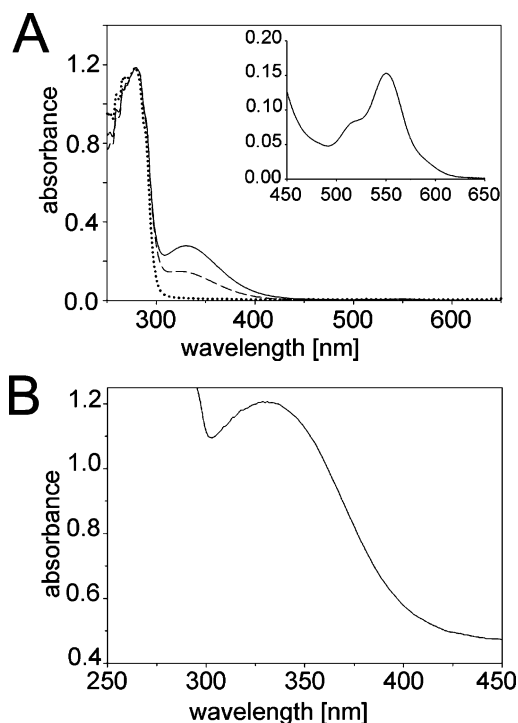


FIGURE 1: hTrx-SNO solution and crystal spectra. (A) Solution absorption spectra of hTrx before (···) and after transnitrosation at pH 7 (---) and pH 9 (—). The A_{280}/A_{335} ratio is consistent with 0, 1, and 2 mol of SNO/mol of protein. The inset shows data for hTrx-SNO (pH 9), highlighting the A_{550} SNO absorption band. (B) Spectra of an hTrx-SNO crystal, displaying a prominent A_{335} SNO absorption band.

iosulfonate (MMTS), followed by reduction and cleavage of the SNO bond with ascorbic acid, biotinylation of the fresh sulfhydryl group, and detection by Western blot analysis. We found hTrx-SNO to be resistant to both the original method (37) and modifications to this method. Ultimately, conditions for specifically labeling a small percentage of the SNO groups in hTrx-SNO by increasing the ascorbic acid concentration 100-fold (to 100 mM) and using 1 mM *N*-ethylmaleimide (NEM) rather than MMTS were identified. Apparently, something about the buried, hydrophobic environments for Cys 62-SNO and Cys 69-SNO in hTrx interfere with the method.

RESULTS

Transnitrosation of hTrx. We incubated recombinant hTrx with GSNO and examined the formation and stability of *S*-nitrosothioredoxin under both analytical (10 μ M hTrx and 50 μ M GSNO) and preparative (1.5 mM hTrx and 15 mM GSNO) conditions, and at two pH values, 7.0 and 9.0. Formation of hTrx-SNO readily occurred under all conditions and was stable for days if the resulting material was stored in the dark and in metal-free buffer. *S*-Nitrosocysteine was quantified using the Saville–Griess assay and absorption spectroscopy (Figure 1). In all cases, ~ 1 mol of SNO/mol of hTrx was found for material prepared at pH 7.0 and ~ 2 mol of SNO/mol of hTrx was found for material prepared at pH 9.0 (Table 1), highlighting the importance of pH and protein environment in the reaction, since hTrx contains five cysteines (Figure 2A). Importantly, essentially identical SNO yields were obtained under both preparative and analytical conditions, consistent with transnitrosation mechanisms

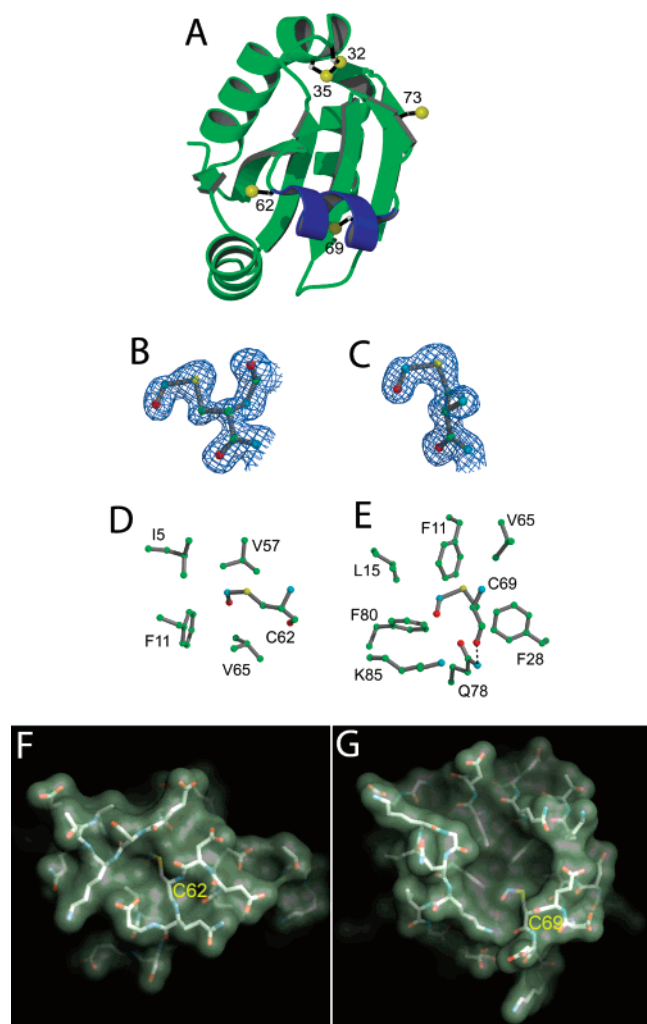


FIGURE 2: hTrx-SNO structure. (A) Ribbon drawing of hTrx indicating cysteine positions and highlighting the helix between Cys 62 and Cys 69. (B and C) Electron density for Cys 62-SNO (molecule C) and Cys 69-SNO (molecule A), respectively. (D and E) Ball-and-stick models for the region surrounding Cys 62-SNO and Cys 69-SNO, which display typical SNO stereochemistry. For Cys 69, the SNO group lies on top of Phe 80 and Phe 11 and the SNO oxygen is near Lys 85 and Gln 78. For Cys 62, the SNO group lies in a hydrophobic pocket formed by the side chains of Ile 5, Phe 11, Val 57, and Val 65 and the backbone of Ser 7. The SNO oxygen is somewhat aligned with the positive (N-terminal) end of the short helix spanning residues 62–69 and may be influenced by the helix dipole. On the surface of the protein, ~ 5 Å from the Cys 62 sulfur, are the carboxylates of Asp 61 and Asp 64. (F and G) Surface views, emphasizing the buried nature of Cys 62-SNO and the hydrophobic pocket for Cys 69-SNO.

occurring in both cases (38), although alternative mechanisms have not yet been ruled out. Others have also reported a maximum transnitrosation of 2 mol of SNO/mol of hTrx (15, 17).

We examined the effect of glutathione on *S*-nitrosothioredoxin by mixing GSNO and thioredoxin in a solution containing 1 mM GSH. Under these conditions, hTrx-SNO was again stable, reaching values after 24 h of ~ 0.3 mol of SNO/mol of hTrx at pH 7 and ~ 0.6 mol of SNO/mol of hTrx at pH 9 (Table 1). These values were independent of which reagent was added first, GSNO or GSH, or temperature (4 or 37 °C), suggesting the system was under thermodynamic control with an equilibrium constant favoring hTrx-SNO over GSNO. This is consistent with hTrx-SNO

measurements in endothelial cells (16). The stability of hemoglobin-SNO to GSH, particularly in the R state, has also been reported (39).

Crystal Structures of hTrx-SNO. We crystallized the purified, transnitrosated protein prepared at two different pH values, leading to three crystal structures. We also examined the protein after peroxide oxidation. Two crystal forms were obtained, a larger cell with three molecules in the asymmetric unit and a smaller cell with one molecule in the asymmetric unit. The best electron density for SNO was obtained from protein transnitrosated at pH 9, crystallized in the larger cell, and measured with a rotating anode X-ray source, yielding a 1.65 Å structure ($R_{\text{cryst}} = 0.19$ and $R_{\text{free}} = 0.24$). All five cysteines were modified in each of the three hTrx molecules, but only two of the five display SNO moieties, Cys 62 and Cys 69 (Figure 2). Cys 32 and Cys 35, which are required for redox activity, are disulfide-linked, and Cys 73 forms an intermolecular disulfide bond with Cys 73 from another hTrx molecule, giving rise to disulfide-linked homodimers similar to those previously described by our group (21, 22). Using synchrotron radiation, diffraction to 1.0 Å was obtained but both SNO and disulfide bonds were photoreduced in the intense synchrotron beam (see Materials and Methods).

The three views of Cys 62-SNO and Cys 69-SNO provide a wealth of new data, with the electron density for Cys 62 (molecule C) and Cys 69 (molecule A) being particularly clear (Figure 2B,C). The protein-SNO stereochemistry is as expected from small-molecule crystal structures (30, 40) (Figure 2D,E), and refinement using small-molecule constraints was well-behaved (Table 3). Three torsional angles, χ_{1-3} , are important in defining the SNO geometry, particularly χ_3 , which defines the rotation about the S–N bond (Table 3). The SNO group is planar due to π orbital conjugation in much the same way as peptide bonds are planar, and χ_3 is therefore restricted to either 0 or 180° (cis or trans, respectively). In general, the SNO groups in hTrx adopt a cis conformation, although Cys 69 (molecule C) displays both cis ($\sim 70\%$) and trans conformers. The values for χ_1 and χ_2 are much less restricted. For χ_1 (rotation about the $\text{C}\alpha\text{--C}\beta$ bond), all of the Cys-SNO groups reside in the most common cysteine rotamer (41), approximately -65° . For χ_2 (rotation about the $\text{C}\beta\text{--S}$ bond), Cys 62 clusters at approximately 180° and Cys 69 at approximately -85° .

Perhaps the most surprising aspect of the SNO-modified molecules is that the Cys 69-SNO is at the bottom of a deep depression (Figure 2G) and the Cys 62-SNO is completely buried and pointing to the protein interior (Figure 2F), placing severe constraints on the transnitrosation reactions at both positions. Both groups form mainly hydrophobic contacts with the protein but lie near hydrophilic side chains (Figure 2D,E). Interestingly, in one recent SNO proteomics study involving tubulin, six of seven nitrosylated cysteines were found to lie in the protein interior (7), and in a second study, SNO modifications were discovered in stretches of hydrophobic amino acids (42). Furthermore, specifically nitrosylated cysteines in hemoglobin, dynamin, and the ryanodine receptor are all thought to reside in hydrophobic environments (reviewed in ref 5). Crystals of hTrx after mutation of Cys 73 to serine and oxidation with hydrogen peroxide diffracted particularly well, providing an excellent model for comparison with hTrx-SNO. This structure, refined to 1.35

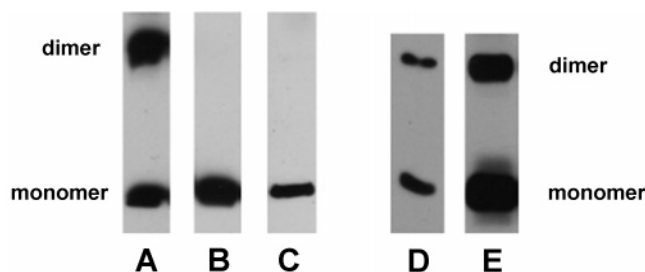


FIGURE 3: Dimer formation and biotin-switch analyses. (A) Western blot (nonreducing) of hTrx-SNO prepared by mixing 10 μ M hTrx with 50 μ M GSNO (pH 7.0) showing formation of a covalently linked dimer. Detection of hTrx in lanes A–C was with an anti-hTrx antibody. (B) hTrx protein without GSNO, showing no dimer formation. (C) hTrx from lysed HT1080 cells, after treatment with 50 μ M GSNO, also showing no dimer formation. (D) Western blot (biotin antibody) of hTrx-SNO [1.5 mM hTrx and 10 mM GSNO (pH 9.0)] after the biotin-switch protocol. Note the very small biotin signal. (E) Like panel D but for unmodified hTrx treated with only biotin. Note the much larger signal and the fact that biotin modification, like GSNO, can also lead to disulfide-linked homodimers. Control biotin-switch experiments conducted in the absence of GSNO did not display any biotin ligation (not shown).

Å resolution ($R_{\text{cryst}} = 0.12$ and $R_{\text{free}} = 0.17$) revealed a fully oxidized Cys 32–Cys 35 disulfide bond and fully reduced Cys 62 and Cys 69 residues. Overall, the mutant structure is very similar to hTrx-SNO but reveals a local expansion at both Cys 62 and Cys 69 upon formation of SNO, and a rotation of the 62–69 intervening helix by ~ 0.5 Å. This helix may move even farther during transnitrosation for GSNO to reach the cysteine residues, particularly buried Cys 62. Importantly, this helix is poorly ordered in molecule B of the hTrx-SNO structure, confirming larger motions are possible, as previously suggested (43).

We also crystallized hTrx-SNO prepared at pH 7 to examine the pH dependence for transnitrosation, leading to a 1.7 Å structure in the smaller unit cell ($R_{\text{cryst}} = 0.21$ and $R_{\text{free}} = 0.24$). We expected Cys 69 to be more readily transnitrosated due to its greater accessibility, its proximity to Lys 85, which could lower its pK_a , and its apparent role in apoptosis (16). However, Cys 69 was largely unmodified at pH 7, while Cys 62 was fully transnitrosated, buried, and in the usual cis geometry.

GSNO-Induced Disulfide Bond Formation. Our data indicate Cys 32 and Cys 73 readily react with GSNO but do not lead to stable adducts. Cys 32 is known to have a reduced pK_a (12), favoring reaction with GSNO, but the modification is readily resolved through reaction with Cys 35, which is in van der Waals contact with Cys 32, leading to disulfide bond formation. This reaction can lead to the direct release of NO from GSNO, which may have additional functional importance (44, 45). Likewise, Cys 73 modification leads to intermolecular disulfide bond formation, at least in vitro (Figure 3A). Homodimerization, however, could not be induced in cell extracts (Figure 3C) and therefore does not appear to occur *in vivo*. Possibly, dimerization is blocked by protein–protein interactions, for example, with apoptosis signal-regulating kinase 1 (ASK1) (46) or thioredoxin binding protein 2 (47) or by glutathionylation at Cys 73 (48). Indeed, the dimerization surface is the same surface that binds peptides from NF κ B and REF-1 (49, 50).

Detecting hTrx-SNO Using the “Biotin-Switch” Protocol. The biotin-switch method is designed to exchange Cys-SNO

conjugates for more stable Cys-S–biotin conjugates that can then be examined by Western blot or mass spectrometry (37) and has become popular for detecting specifically nitrosated proteins in complex mixtures. In anticipation of such experiments involving hTrx, we sought to characterize hTrx-SNO using the biotin-switch approach. In our hands, we found Cys 62-SNO and Cys 69-SNO to be resistant to the biotin-switch protocol, even with purified material that exhibited clear modifications by spectroscopy, Saville–Griess, and crystallography (Figure 3D). This difficulty is possibly related to the buried nature of the SNO groups in hTrx. Detection was enhanced (but still weak) after modification of the procedure to use excess reductant (100 mM ascorbate acid) and a more potent methylating agent (*N*-ethylmaleimide).

DISCUSSION

Protein S-nitrosation is implicated in numerous physiological processes; however, the biochemistry behind these events is unclear, and structural data are virtually nonexistent. To begin filling this gap, we examined GSNO transnitrosation of human thioredoxin, a protein implicated in several SNO signaling and metabolism pathways. Using physiologically relevant concentrations of GSNO, we detected one SNO moiety per hTrx molecule for reactions at pH 7.0 and two SNO moieties per hTrx molecule at pH 9.0 (Table 1). No transnitrosation was detected at pH 5.6. These modifications were relatively stable, even in the presence of 1 mM glutathione, a concentration similar to that found in eukaryotic cells.

We determined crystal structures of hTrx-SNO to reveal which of the five cysteines were modified and to uncover factors of importance to SNO formation and stability. Surprisingly, the most buried cysteine, Cys 62, forms the most stable SNO adduct: crystal structures of hTrx-SNO prepared at pH 7.0 revealed a Cys 62-SNO modification, while protein prepared at pH 9.0 revealed Cys 62-SNO and Cys 69-SNO modifications (Figure 2). The SNO groups in these structures in general adopt cis planar geometries and display good stereochemistry (Table 3). The helix intervening between Cys 62 and Cys 69 rotates outward by ~ 0.5 Å to accommodate the SNO groups. The remaining cysteines in the protein form intramolecular disulfide bonds (Cys 32–Cys 35) or intermolecular disulfide bonds (Cys 73).

Transnitrosation Models. Taken together, our data suggest a new mechanism for stable transnitrosation of hTrx and possibly many other proteins (Figure 4). In this model, SNO exchange takes place in a protected pocket where the leaving and forming SNO groups can simultaneously adopt planar geometries, and where intermediate charge buildup can be stabilized. GSNO is expected to bind to the protein with its SNO group in the trans isomer, which alleviates steric conflict with the protein. Binding of the hydrophobic SNO group is into a hydrophobic pocket made accessible through dynamic fluctuations in the helix of residues 62–69 (described above) and oriented such that the SNO π^* orbital is aligned for reacting with the protein’s cysteine. Some means of reducing the cysteine pK_a , normally ~ 8.5 , would enhance thiolate anion formation and nucleophilic attack. Local protein environments can readily accomplish this; for example, thymidylate synthase, which undergoes addition

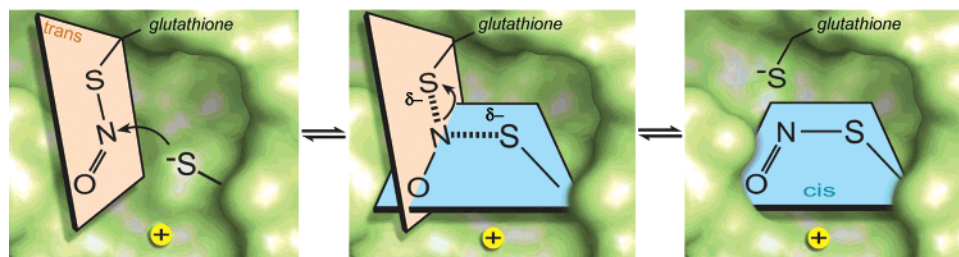


FIGURE 4: Possible mechanism for S-nitrosylation of hTrx. In the left panel, GSNO is expected to bind to the protein with its SNO group in the trans isomer. In the middle panel is stabilization of a nitroxyl disulfide intermediate. In the right panel, release of the SNO group into a hydrophobic pocket would stabilize the protein-SNO product. See the text for additional details.

of cysteine to deoxyuridine monophosphate (dUMP), stabilizes the thiolate anion through direct contact with an invariant arginine (51, 52). For hTrx, Cys 69, which does not react with GSNO at pH 7, appears not to have a perturbed pK_a despite the nearby Lys 85 (Figure 2e), while Cys 62, which reacts well with GSNO at pH 7, may have a pK_a that is reduced through interaction with the nearby helix dipole, despite the relative proximity to Glu 6, Asp 61, and Asp 64 (not shown).

Stabilization of the most likely intermediate would facilitate the reaction. The best geometry would be one in which the developing and breaking S–N bonds are arranged tetrahedrally around the central nitrogen atom with planar SNO conformations. This arrangement, termed a nitroxyl disulfide, has been modeled computationally, leading to a predicted transition state with most of the charge residing on the sulfur atoms, rather than on the SNO oxygen (53). Stabilization of the negative charge on the intermediate would also be beneficial and might occur through Lys 85 (Cys 69) and the helix dipole of residues 62–69 (Cys 62).

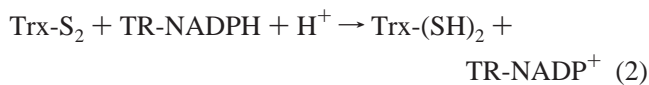
Placement of the SNO group into a hydrophobic pocket would stabilize the protein-SNO product. The geometric constraints of a trans GSNO group reacting with cysteine in the fixed protein pocket, and the nitroxyl disulfide arrangement described above, would lead to a cis SNO conformation in the product. Interestingly, both Cys 69-SNO and Cys 62-SNO display cis conformers (Figure 2 and Table 3). However, whether this occurs because isomerization is slow or because the cis conformer is more stable for these groups is not yet clear. For small molecules in solution, the energetic barrier to cis–trans isomerization is ~ 12 kcal/mol (30, 31), a value consistent with isomerization on the millisecond time scale. However, in the protein, isomerization rates may be severely modified due to steric constraints.

Several alternative nitrosation–nitrosylation mechanisms for protein thiols, some involving S-nitrosylation motifs, have been proposed (see ref 5 for a recent review). One attractive proposal is the use of acid–base chemistry in SNO exchange, with base removal of a proton from the attacking thiol, and acid protonation of the resulting thiolate anion (5, 54, 55). To be efficient, such a mechanism would require a precise alignment of the reacting groups and precise matching of pK_a values as typically found in enzyme active sites, but such an arrangement is not present in our structures and appears unlikely to occur in hTrx. Likewise, a more complicated mechanism involving release of NO from GSNO followed by direct cysteine nitrosylation to give the thionitroxide (SNO[−]), followed by oxidation to give SNO, can be envisioned on the basis of computational and biochemical

studies described for hemoglobin (10, 56). In particular, since both NO and O₂ preferably partition into hydrophobic environments, such a mechanism might lead to nitrosylation of buried thiols (5). However, in preliminary experiments, NO alone does not lead to hTrx-SNO formation in our hands, so this mechanism seems to be precluded in this study. Finally, we have assumed that transnitrosation at Cys 62 and Cys 69 occurs through GSNO, but it remains possible that the initial transnitrosation might take place on a different cysteine, for example, Cys 73, followed by a second transnitrosation onto the final groups. This possibility is currently under investigation.

Protein–Protein Transnitrosation. That hTrx is readily and stably S-nitrosated in our hands is consistent with previous studies showing that hTrx-SNO interferes with apoptosis (16, 17) and can transnitrosate caspase-3 in vitro (18). However, certain details differ between those studies and the work presented here. In the in vivo studies, Cys 69 was identified as being key for anti-apoptotic activity; however, cysteines 62 and 73 were not examined, and a His-tagged version of the protein was employed (16, 17). In the in vitro study, transfer to caspase-3 was shown to involve Cys 73 through mutagenesis and mass spectrometry after the SNO group is exchanged for biotin. This study differed from ours in that a His-tagged protein was used for some of the work, a 10-fold higher GSNO concentration was employed, and incubation took place at 37 °C instead of 25 °C. In our hands, with the untagged protein, Cys 73 becomes disulfide-linked, a reaction that appears to be prevented in vivo (Figure 3), and Cys 69 is poorly nitrosated at pH 7.0 but readily nitrosated at pH 9.0. Taken together, it seems clear that all three cysteines are capable of transnitrosation activities but that the conditions that are employed affect the outcome (e.g., tagged or untagged protein, pH, temperature, GSNO concentration, in vivo or in vitro, etc.). Additional studies aimed at examining the roles of these factors in hTrx function are underway.

Mammalian thioredoxins are highly conserved, being 75% identical among species ranging from mice to humans, and are particularly conserved near the five cysteines in question. This high degree of conservation suggests all five cysteines may have functional roles *in vivo*, possibly providing specificity for transnitrosation reactions with other proteins. The best characterized of these are the oxidoreductase activities of Cys 32 and Cys 35, which are capable of reducing oxidized cysteines on other proteins. Here, we show that reaction with GSNO leads to formation of a Cys 32–Cys 35 disulfide bond, suggesting the following reaction scheme may occur in vivo:



where RSNO is an S-nitrosylated protein, Trx-(SH)₂ is reduced thioredoxin, Trx-S₂ is oxidized thioredoxin, and TR is NADPH-dependent thioredoxin reductase. In this way, thioredoxin might be involved in the removal of SNO groups from proteins in much the same way that it reduces disulfide bonds.

The surfaces surrounding the three remaining cysteines may dictate their roles in reactions between proteins. Transnitrosation reactions between hTrx-Cys 73 and the caspase-3 catalytic cysteine (Cys 163) are perhaps facilitated by their complementary shapes: Cys 73 protrudes from the hTrx protein surface, and the caspase-3 sulfhydryl lies within an active site pocket (18). Cys 69-SNO also appears to be important in apoptosis and is S-nitrosylated *in vivo* (16, 17) but is only marginally S-nitrosated by GSNO at neutral pH in our hands. Although a mechanism for Cys 69-dependent anti-apoptosis activity has not yet been identified, it was proposed that the role of Cys 69-SNO was to modulate hTrx catalytic activity (16, 17). It should also be noted that those experiments demonstrating cardioprotective effects of hTrx (16, 17) are likely to have also included Cys 62-SNO, which is difficult to detect using a conventional methodology (Figure 3) but readily apparent in our crystal structures (Figure 2b). A physiological role for the Cys-62 SNO group discovered here awaits further study, but in preliminary experiments, it appears to be capable of transnitrosating at least one of the 37 cysteines in human sGC (X. Hu and W. R. Montfort, unpublished data) and may provide for great specificity in transnitrosation reactions due to its buried state.

In summary, we have determined the first structure of a transnitrosated protein, hTrx-SNO, which displays an unexpected buried SNO moiety. The results suggest a new mechanism for transnitrosation reactions and further solidify a role for human thioredoxin in SNO signaling and metabolism.

ACKNOWLEDGMENT

We thank Abreeza Zegeer for excellent crystal preparation, Cheryl Ryan for help with Figure 4, and Dr. Joseph Bonaventura and the COBRE II Protein Center for help with transnitrosation experiments while W.R.M. was on sabbatical at the University of Puerto Rico, Mayagüez, PR. We also thank Dr. Roger Miesfeld and Susan Kunz for help with HT1080 cell growth and Dr. Richard Glass for mechanistic insight.

REFERENCES

- Ignarro, L. J. (2000) *Nitric Oxide Biology and Pathobiology*, Academic Press, San Diego.
- Levy, R. M., Prince, J. M., and Billiar, T. R. (2005) Nitric oxide: A clinical primer, *Crit. Care Med.* 33, S492–S495.
- Uehara, T., Nakamura, T., Yao, D., Shi, Z. Q., Gu, Z., Ma, Y., Masliah, E., Nomura, Y., and Lipton, S. A. (2006) S-Nitrosylated protein-disulphide isomerase links protein misfolding to neurodegeneration, *Nature* 441, 513–517.
- Cary, S. P., Winger, J. A., Derbyshire, E. R., and Marletta, M. A. (2006) Nitric oxide signaling: No longer simply on or off, *Trends Biochem. Sci.* 31, 231–239.
- Hess, D. T., Matsumoto, A., Kim, S. O., Marshall, H. E., and Stamler, J. S. (2005) Protein S-nitrosylation: Purview and parameters, *Nat. Rev. Mol. Cell Biol.* 6, 150–166.
- Jia, L., Bonaventura, C., Bonaventura, J., and Stamler, J. S. (1996) S-Nitrosohaemoglobin: A dynamic activity of blood involved in vascular control, *Nature* 380, 221–226.
- Hao, G., Derakhshan, B., Shi, L., Campagne, F., and Gross, S. S. (2006) SNOSID, a proteomic method for identification of cysteine S-nitrosylation sites in complex protein mixtures, *Proc. Natl. Acad. Sci. U.S.A.* 103, 1012–1017.
- Weichsel, A., Maes, E. M., Andersen, J. F., Valenzuela, J. G., Shokhireva, T., Walker, F. A., and Montfort, W. R. (2005) Heme-assisted S-nitrosation of a proximal thiolate in a nitric oxide transport protein, *Proc. Natl. Acad. Sci. U.S.A.* 102, 594–599.
- Chan, N. L., Kavanaugh, J. S., Rogers, P. H., and Arnone, A. (2004) Crystallographic analysis of the interaction of nitric oxide with quaternary-T human hemoglobin, *Biochemistry* 43, 118–132.
- Zhao, Y. L., and Houk, K. N. (2006) Thionitroxides, RSNHO*: The Structure of the SNO Moiety in “S-Nitrosohemoglobin”, A Possible NO Reservoir and Transporter, *J. Am. Chem. Soc.* 128, 1422–1423.
- Arner, E. S., and Holmgren, A. (2000) Physiological functions of thioredoxin and thioredoxin reductase, *Eur. J. Biochem.* 267, 6102–6109.
- Powis, G., and Montfort, W. R. (2001) Properties and biological activities of thioredoxins, *Annu. Rev. Pharmacol. Toxicol.* 41, 261–295.
- Burke-Gaffney, A., Callister, M. E., and Nakamura, H. (2005) Thioredoxin: Friend or foe in human disease? *Trends Pharmacol. Sci.* 26, 398–404.
- Matsui, M., Oshima, H., Takaku, K., Maruyama, T., Yodoi, J., and Taketo, M. M. (1996) Early embryonic lethality caused by targeted disruption of the mouse thioredoxin gene, *Dev. Biol.* 178, 179–185.
- Sumbayev, V. V. (2003) S-Nitrosylation of thioredoxin mediates activation of apoptosis signal-regulating kinase 1, *Arch. Biochem. Biophys.* 415, 133–136.
- Haendeler, J., Hoffmann, J., Tischler, V., Berk, B. C., Zeiher, A. M., and Dimmeler, S. (2002) Redox regulatory and anti-apoptotic functions of thioredoxin depend on S-nitrosylation at cysteine 69, *Nat. Cell Biol.* 4, 743–749.
- Tao, L., Gao, E., Bryan, N. S., Qu, Y., Liu, H. R., Hu, A., Christopher, T. A., Lopez, B. L., Yodoi, J., Koch, W. J., Feelisch, M., and Ma, X. L. (2004) Cardioprotective effects of thioredoxin in myocardial ischemia and reperfusion: Role of S-nitrosation [corrected], *Proc. Natl. Acad. Sci. U.S.A.* 101, 11471–11476.
- Mitchell, D. A., and Marletta, M. A. (2005) Thioredoxin catalyzes the S-nitrosation of the caspase-3 active site cysteine, *Nat. Chem. Biol.* 1, 154–158.
- Liu, L., Hausladen, A., Zeng, M., Que, L., Heitman, J., and Stamler, J. S. (2001) A metabolic enzyme for S-nitrosothiol conserved from bacteria to humans, *Nature* 410, 490–494.
- Zhang, Y., and Hogg, N. (2004) Formation and stability of S-nitrosothiols in RAW 264.7 cells, *Am. J. Physiol.* 287, L467–L474.
- Andersen, J. F., Sanders, D. A. R., Gaskaska, J. R., Weichsel, A., Powis, G., and Montfort, W. R. (1997) Human thioredoxin homodimers: Regulation by pH, role of Asp 60, and crystal structure of the Asp 60 → Asn mutant, *Biochemistry* 36, 13979–13988.
- Weichsel, A., Gaskaska, J. R., Powis, G., and Montfort, W. R. (1996) Crystal structures of reduced, oxidized, and mutated human thioredoxins: Evidence for a regulatory homodimer, *Structure* 4, 735–751.
- Hart, T. W. (1985) Some observations concerning the S-nitroso and S-phenylsulphonyl derivatives of L-cysteine and glutathione, *Tetrahedron Lett.* 26, 2013–2016.
- Saville, B. (1958) A scheme for the colorimetric determination of microgram amounts of thiols, *Analyst (Cambridge, U.K.)* 83, 670–672.
- Schmidt, H. H. W., and Kelm, M. (1996) Determination of Nitrite and Nitrate by the Griess Reaction, in *Methods in Nitric Oxide Research* (Feelisch, M., and Stamler, J. S., Eds.) pp 491–497, John Wiley & Sons, Ltd., Chichester, U.K.
- Dasgupta, T. P., and Smith, J. N. (2002) Reactions of S-nitrosothiols with L-ascorbic acid in aqueous solution, *Methods Enzymol.* 359, 219–229.

27. Pflugrath, J. W. (1999) The finer things in X-ray diffraction data collection, *Acta Crystallogr. D55*, 1718–1725.
28. Collaborative Computational Project Number 4 (1994) The CCP4 Suite: Programs for Protein Crystallography, *Acta Crystallogr. D50*, 760–763.
29. Emsley, P., and Cowtan, K. (2004) Coot: Model-building tools for molecular graphics, *Acta Crystallogr. D60*, 2126–2132.
30. Arulsamy, N., Bohle, D. S., Butt, J. A., Irvine, G. J., Jordan, P. A., and Sagan, E. (1999) Interrelationships between conformational dynamics and the redox chemistry of S-nitrosothiols, *J. Am. Chem. Soc.* 121, 7115–7123.
31. Bartberger, M. D., Houk, K. N., Powell, S. C., Mannion, J. D., Lo, K. Y., Stamler, J. S., and Toone, E. J. (2000) Theory, spectroscopy, and crystallographic analysis of S-nitrosothiols: Conformational distribution dictates spectroscopic behavior, *J. Am. Chem. Soc.* 122, 5889–5890.
32. Iulek, J., Alphey, M. S., Westrop, G. D., Coombs, G. H., and Hunter, W. N. (2006) High-resolution structure of recombinant *Trichomonas vaginalis* thioredoxin, *Acta Crystallogr. D62*, 216–220.
33. Kraulis, P. J. (1991) MOLSCRIPT: A program to produce both detailed and schematic plots of protein structures, *J. Appl. Crystallogr.* 24, 946–950.
34. Esnouf, R. M. (1997) An extensively modified version of MolScript that includes greatly enhanced coloring capabilities, *J. Mol. Graphics Modell.* 15, 132–134, 112–113.
35. Merritt, E. A., and Murphy, M. E. P. (1994) Raster3D Version 2.0: A Program for Photorealistic Molecular Graphics, *Acta Crystallogr. D50*, 869–873.
36. Chauhan, S., Pandey, R., Way, J. F., Sroka, T. C., Demetriou, M. C., Kunz, S., Cress, A. E., Mount, D. W., and Miesfeld, R. L. (2003) Androgen regulation of the human FERM domain encoding gene EHM2 in a cell model of steroid-induced differentiation, *Biochem. Biophys. Res. Commun.* 310, 421–432.
37. Jaffrey, S. R., and Snyder, S. H. (2001) The biotin switch method for the detection of S-nitrosylated proteins, *Sci. STKE* 2001, PL1.
38. Williams, D. L. H. (1996) S-Nitrosothiols and Role of Metal Ions in Decomposition to Nitric Oxide, *Methods Enzymol.* 268, 299–308.
39. McMahon, T. J., Stone, A. E., Bonaventura, J., Singel, D. J., and Stamler, J. S. (2000) Functional coupling of oxygen binding and vasoactivity in S-nitrosohemoglobin, *J. Biol. Chem.* 275, 16738–16745.
40. Yi, J., Khan, M. A., Lee, J., and Richter-Addo, G. B. (2005) The solid-state molecular structure of the S-nitroso derivative of L-cysteine ethyl ester hydrochloride, *Nitric Oxide* 12, 261–266.
41. Lovell, S. C., Word, J. M., Richardson, J. S., and Richardson, D. C. (2000) The penultimate rotamer library, *Proteins* 40, 389–408.
42. Greco, T. M., Hodara, R., Parastatidis, I., Heijnen, H. F., Dennehy, M. K., Liebler, D. C., and Ischiropoulos, H. (2006) Identification of S-nitrosylation motifs by site-specific mapping of the S-nitrosocysteine proteome in human vascular smooth muscle cells, *Proc. Natl. Acad. Sci. U.S.A.* 103, 7420–7425.
43. Watson, W. H., Pohl, J., Montfort, W. R., Stuchlik, O., Reed, M. S., Powis, G., and Jones, D. P. (2003) Redox potential of human thioredoxin 1 and identification of a second dithiol/disulfide motif, *J. Biol. Chem.* 278, 33408–33415.
44. Nikitovic, D., and Holmgren, A. (1996) S-Nitrosoglutathione is cleaved by the thioredoxin system with liberation of glutathione and redox regulating nitric oxide, *J. Biol. Chem.* 271, 19180–19185.
45. Sliskovic, I., Raturi, A., and Mutus, B. (2005) Characterization of the S-denitrosation activity of protein disulfide isomerase, *J. Biol. Chem.* 280, 8733–8741.
46. Saitoh, M., Nishitoh, H., Fujii, M., Takeda, K., Tobiume, K., Sawada, Y., Kawabata, M., Miyazono, K., and Ichijo, H. (1998) Mammalian thioredoxin is a direct inhibitor of apoptosis signal-regulating kinase (ASK) 1, *EMBO J.* 17, 2596–2606.
47. Nishiyama, A., Matsui, M., Iwata, S., Hirota, K., Masutani, H., Nakamura, H., Takagi, Y., Sono, H., Gon, Y., and Yodoi, J. (1999) Identification of thioredoxin-binding protein-2/vitamin D₃ up-regulated protein 1 as a negative regulator of thioredoxin function and expression, *J. Biol. Chem.* 274, 21645–21650.
48. Casagrande, S., Bonetto, V., Fratelli, M., Gianazza, E., Eberini, I., Massignan, T., Salmona, M., Chang, G., Holmgren, A., and Ghezzi, P. (2002) Glutathionylation of human thioredoxin: A possible crosstalk between the glutathione and thioredoxin systems, *Proc. Natl. Acad. Sci. U.S.A.* 99, 9745–9749.
49. Qin, J., Clore, G. M., Kennedy, W. P., Kuszewski, J., and Gronenborn, A. M. (1996) The solution structure of human thioredoxin complexed with its target from Ref-1 reveals peptide chain reversal, *Structure* 4, 613–620.
50. Qin, J., Clore, G. M., Kennedy, W. P., Huth, J. R., and Gronenborn, A. M. (1994) Solution structure of human thioredoxin in a mixed disulfide intermediate complex with its target peptide from the transcription factor NFκB, *Structure* 3, 289–297.
51. Sotelo-Mundo, R. R., Changchien, L., Maley, F., and Montfort, W. R. (2006) Crystal structures of thymidylate synthase mutant R166Q: Structural basis for the nearly complete loss of catalytic activity, *J. Biochem. Mol. Toxicol.* 20, 88–92.
52. Finer-Moore, J. S., Santi, D. V., and Stroud, R. M. (2003) Lessons and conclusions from dissecting the mechanism of a bisubstrate enzyme: Thymidylate synthase mutagenesis, function, and structure, *Biochemistry* 42, 248–256.
53. Houk, K. N., Hietbrink, B. N., Bartberger, M. D., McCarren, P. R., Choi, B. Y., Voyksner, R. D., Stamler, J. S., and Toone, E. J. (2003) Nitroxyl disulfides, novel intermediates in transnitrosation reactions, *J. Am. Chem. Soc.* 125, 6972–6976.
54. Stamler, J. S., and Hausladen, A. (1998) Oxidative modifications in nitrosative stress, *Nat. Struct. Biol.* 5, 247–249.
55. Ascenzi, P., Colasanti, M., Persichini, T., Muolo, M., Polticelli, F., Venturini, G., Bordo, D., and Bolognesi, M. (2000) Re-evaluation of amino acid sequence and structural consensus rules for cysteine-nitric oxide reactivity, *Biol. Chem.* 381, 623–627.
56. Singel, D. J., and Stamler, J. S. (2005) Chemical physiology of blood flow regulation by red blood cells: The role of nitric oxide and S-nitrosohemoglobin, *Annu. Rev. Physiol.* 67, 99–145.

BI061878R